Sub Topic: Fire Research

12th U. S. National Combustion Meeting
Organized by the Eastern States Section of the Combustion Institute
May 24–26, 2021
College Station, Texas

Examining the effect of fire retardant on the combustion of wood via X-ray Computed Tomography

Emeric Boigné[1,], N. Robert Bennett[2], Adam Wang[2], Matthias Ihme[1]*

[1]Department of Mechanical Engineering, Stanford University, Stanford, CA 94305
[2]Department of Radiology, Stanford University, Stanford, CA 94305
[*]Corresponding Author Email: eboigne@stanford.edu

Abstract: Fire retardants are used to slow down the spread of wildfires or reduce the flammability of manufactured materials such as plastics and textiles. The chemical pathways for retardant quenching are well understood, and standard flame resistance tests are routinely performed for flammability certification. However, these tests are often limited to measurements of ignition time and global flame spread under different fire conditions. As such, they do not provide detailed information on the local combustion processes. Acquiring detailed fire measurements in-situ remains challenging, mainly because of the multiphase nature of solid fuel combustion and the associated release of smoke and tar. To address these challenges, X-ray Computed Tomography (XCT) with simultaneous gas and solid measurements was recently proposed as an in-situ imaging technique for solid fuel combustion. This method provides measurements of both the gas temperature and the structural changes occurring inside solid fuel during combustion. In the present work, simultaneous XCT is employed to examine the pyrolysis and flame spread for untreated wood samples, and for wood samples treated with Phos-Chek fire retardant, a formulation commonly used in wildfires applications. The time-resolved 3D results provide detailed measurements of the charring and oxidation occurring within the fuel, thus highlighting how fire retardant affect these mechanisms.
Keywords: Wildfires, Fire retardant, X-ray computed tomography

1. Introduction

Wildfires represent an important environmental hazard that accelerates climate change. Last year, widespread Australian bushfires injected amounts of smoke into the stratosphere equivalent to those from a moderate volcanic eruption [1]. To address this growing challenge, prescribed burns can be deployed to mitigate the risk of catastrophic wildfires [2], whereas Fire Retardants (FRs) can help suppress widespread. Although FRs are generally dropped from aircraft or applied by ground crews during firefighting, the prophylactic treatment of high-risk landscapes has also been recently proposed [3]. FRs usually consist of a mixture of water and chemicals. The same chemical agents are used in flame retardants for manufactured materials [4]. Halogens were a common choice at first, while organic and inorganic compounds are now preferred due to their reduced toxicity. For instance, inorganic ammonium polyphosphate (APP) is the primary chemical agent of Phos-Chek, a commercial FR widely used by firefighters in North America.

The fire suppression from APP relies on physical and chemical mechanisms acting in both the gas and condensed phases. In the solid phase, the heating of APP above 280 °C results in the formation of a protective surface coating of polyphosphoric acid [4, 5, 6, 7]. This acid acts as a

catalyzer for the dehydration of the numerous hydroxyl groups found in the organic polymers comprising wood, such as cellulose and hemicellulose. Specifically, the acid reacts with hydroxyl groups to form phosphate esters, which decomposes under heat exposure releasing water while regenerating the acid catalyzer [4, 7]. The carbon char resulting from this catalysis reaction is a high temperature resistant graphite-like char, which inhibits the transport of heat and O_2 within the cellulosic fuel. The intumescent growth of this protective char layer can be further promoted when a nitrogen blowing agent is present, for instance melanin [4, 7, 8]. At temperatures above 550 °C, the polyphosphoric acid is further dehydrated to P_4O_{10} whose sublimation acts as a heat sink [5, 6, 7]. In the gas phase, free PO radicals can quench the chain reaction, and inhibit stable flame formation [4, 8]. In addition, the water vapor released by the catalysis reaction further dilute the flammable pyrolyzate gases, thereby reducing the flaming intensity.

In order to evaluate the efficacy of FRs and certify material flammability, several standard tests are routinely performed [4]. For instance, in cone calorimetry experiments, the material response to radiant heating is investigated, whereas measurements of limited oxygen index evaluate the minimum oxygen content needed to sustain a flame. In these tests, the efficacy of FRs is evaluated by characterizing the flaming ignition or reporting global measurements such as total mass-loss. However, only limited investigations have focused on provided detailed measurements of the effect of FR on wood combustion. This trend is in part due to the challenges associated with acquiring detailed multiphase measurements in fire experiments, such as the release of smoke and tar. We recently demonstrated that X-ray Computed Tomography (XCT) can be employed to acquire detailed simultaneous measurements of solid density and gas temperature during combustion [9]. To achieve gas temperature measurements using XCT, the gas flow is diluted with Kr, a high-contrast agent [10].

In the present work, XCT is utilized to examine in-situ the effect of FR on the combustion of birch wood. Cubic samples are heated by radiation and convection in a confined flow of N_2, O_2, and Kr. XCT measurements of gas temperature and solid density are acquired in-situ to investigate the combustion of samples coated with Phos-Chek FR. Results with uncoated samples are compared to analyze the fire suppression mechanisms occurring within the solid fuel.

2. Experimental Methods

In this work, XCT was employed to measure the 3D field of density ρ inside the solid sample and the surrounding gas phase. Specifically, XCT measured the X-ray linear attenuation $\mu = \rho\zeta$ at a spatial resolution of about 300 μm and a temporal resolution of 90 s. The mass-attenuation coefficients relating the linear attenuation and density were measured by calibration. To achieve sufficient attenuation in the gas-phase and enable temperature measurements, the flow was diluted with Kr. Further details on the technique are available in previous publications [9, 10].

The experimental setup and samples used are presented in Figure 1. A thermocouple held cubic birch samples of 16 mm size inside of a quartz tube with a vertical flow of N_2, O_2, and Kr. The mixture was flown at a constant upward velocity of 1.89 ± 0.08 cm/s. The concentration of N_2 and O_2 was varied to control the oxygen content, whereas the Kr concentration was kept at 50% per volume. A flat coil heater was placed upstream of the sample to provide heating by radiation and convection. The heating by radiation was estimated to 5.23 kW/m² at the lower surface of the sample. The quartz tube apparatus was placed on the rotation stage of a laboratory XCT scanner.

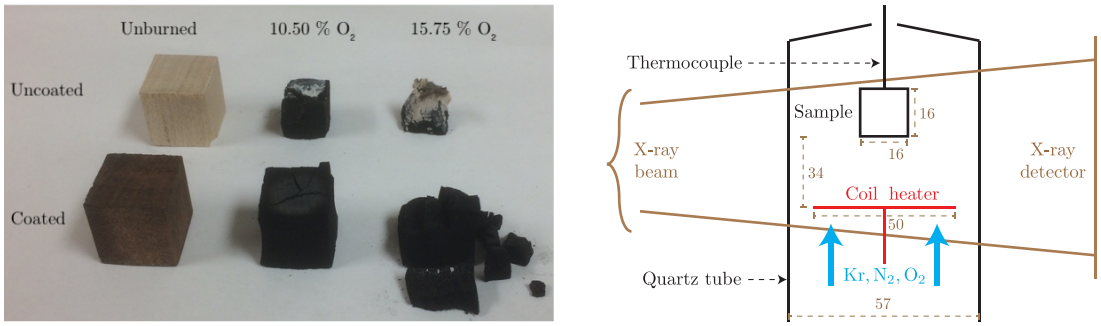

Figure 1: Picture of birch samples used (left), and schematic of experimental setup with dimensions in mm (right).

To measure in-situ the gas temperature and solid density, successive XCT scans were acquired during combustion of the sample. The sample was placed inside the tube at time 00:00 to start each run, after stabilization of the flow and heater. XCT scans were then acquired approximately every 90 s, each scan lasting 30 s. The experiments were stopped at time 16:00 by turning off the heater.

The birch samples were machined from commercial lumber and operated so that the wood grain was aligned with the vertical direction. To simulate FR treatment, the samples were submerged in a bath of Phos-Chek LC95A for 10 s. Both the coated and uncoated samples were then dried at 110 °C for three hours. According to the manufacturer 2020 safety data sheet, Phos-Chek LC95A consists of an APP solution (>80%), iron oxide (<5%), attapulgus clay (<5%), and trade-secret performance additives (5–10%).

3. Results and Discussion

Using both coated and uncoated samples, three different oxygen concentrations were compared: 10.50%, 15.75%, and 21.00% per-volume. Gas-phase ignition was observed 2–5 minutes after the beginning of each run. This flaming was sustained for about 5 minutes, after which a smoldering regime took over. The intensity of the char oxidation during smoldering was particularly affected by the oxygen concentration. Overall, FR coating led to a slight delay in ignition time, a relatively unaffected pyrolysis, a slightly lower amount of heat released during flaming, but a significantly reduced intensity in char oxidation.

XCT results are provided in Figure 2, comparing conditions with 21% oxygen for coated and uncoated samples. It shows vertical cross-sections of solid density and gas temperature at a slice taken 2 mm away from the centerline to highlight crack formation, and char oxidation within the char. In both cases, the pyrolysis completed within 7 minutes, after which the flames extinguished, and smoldering took over. Although similar behaviors are observed during flaming for both samples, the results highlight large differences during the char oxidation. For the uncoated samples, the smoldering occurs both on the lateral sides and the lower surface of the sample, progressively consuming the sample from the outside until a large vertical crack is formed inside the sample. In contrast, for the sampled coated with FR, a protective char layer forms on the outer surface inhibiting the char oxidation. Significant char oxidation is only observed at the position shown, 2 mm away from the centerline. In this case, the smoldering front penetrates through the protective layer locally, before propagating within the sample.

To further quantify the pyrolysis and oxidation rates, Figure 3 presents volume-averaged measurements of the reaction rates of pyrolysis and char oxidation, along with thermocouple

readings. The individual reaction rates were evaluated from the solid density measurements and indicate the heat contribution of the reactions to the total heat release rate [10]. These quantitative results further confirm the similarities observed during flaming, although lower temperatures and delayed ignition are highlighted. Larger differences are seen in the char oxidation results, for which the total time-integrated char oxidation is reduced for the coated samples by a factor of 1.8x (10.50% O_2) to 2.6x (21% O_2). Specifically, the oxidation reduction remains limited during flaming, but is significant once the pyrolysis ends. For instance, at 15.75% O_2, less than 0.01 g/min of char oxidation is measured with FR coating after flaming, whereas rates of up to 0.07 g/min are measured for uncoated samples. At 21% O_2, the local char oxidation within the sample visible in Figure 2 explains the oxidation rate of up to 0.02 g/min measured post-flaming.

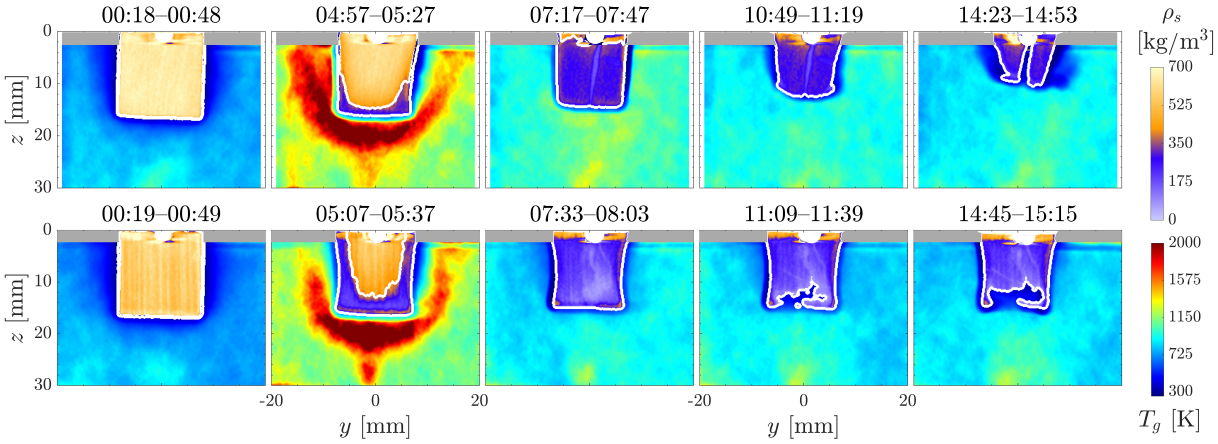

Figure 2: XCT cross-sections of solid density ρ_s and gas temperature T_g taken at x=2 mm for (top) uncoated samples and (bottom) coated samples operated at 21% oxygen.

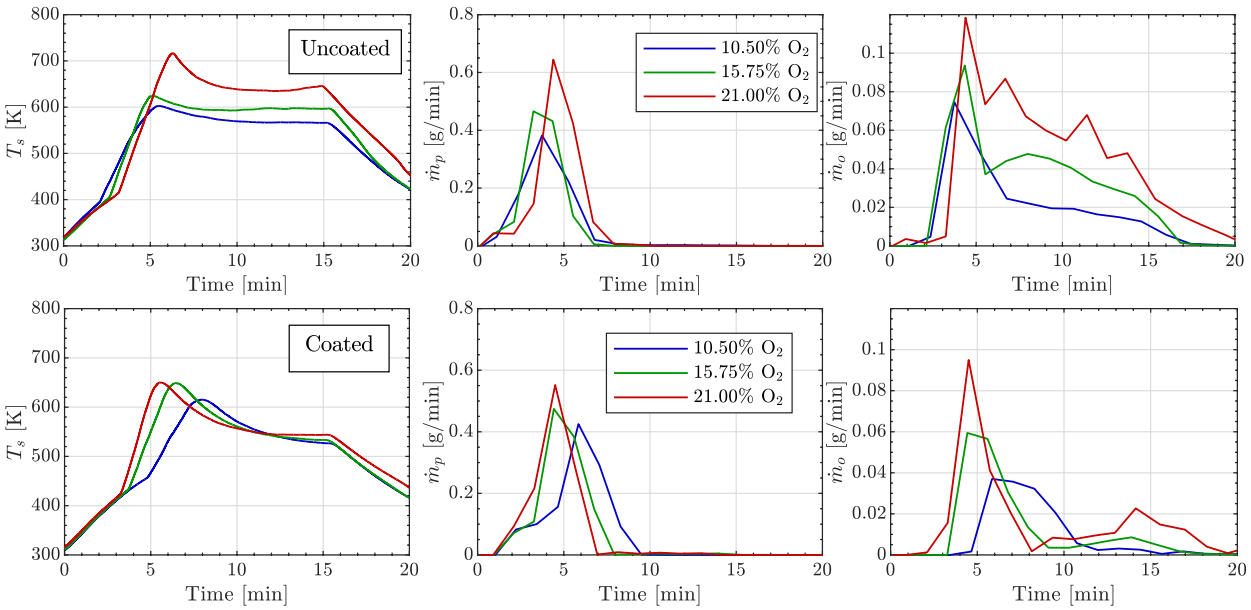

Figure 3: Time evolutions of (left) thermocouple measurements, (center) pyrolysis reaction rates, and (right) char oxidation reaction rates for (top) uncoated samples and (bottom) coated samples.

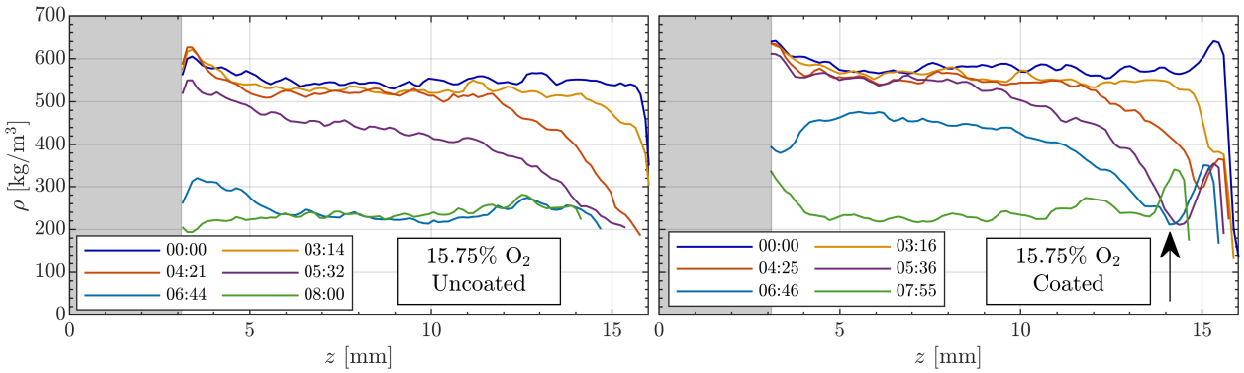

Figure 4: Line profiles of solid density along the vertical direction z for different times comparing cases (left) without fire retardant and (right) with fire retardant at 15.75% O_2. The scans after 8:00 only featured minor variations in density and are thus not shown.

Although the protective coating near the surface of the sample is marked with a slightly higher density, it is not so visible for the coated sample shown in Figure 2. To highlight this protective layer, Figure 4 presents lines profiles of solid density along the vertical direction for cases with 15.75% O_2. In Figure 4, a black arrow highlights the local increase in density near the surface of the coated sample, unseen in the uncoated sample. Note that this peak is also visible in the scan acquired before combustion (time 00:00), indicating that the FR coating locally increases the X-ray attenuation at the surface. However, the combustion does not reduce the height of this peak, suggesting that large amounts of FR compounds are still present after flaming, despite the important local heating. In fact, gaseous ammonia is released at temperatures of about 550 K, whereas the sublimation of the phosphate requires temperature of up to 820 K [4, 5, 6, 7]. Although the thermocouple readings reported in Figure 3 only provide volume-averaged measurements of the solid temperature, the values measured suggest the dehydration of APP into phosphoric acid, the release of gaseous ammonia, but not the sublimation of the phosphate into PO quenching radicals at the conditions investigated. This analysis is consistent with the experimental results highlighting a limited impact of the FR coating on the flaming regime, but a highly effective reduction of the char oxidation.

4. Conclusions

In this work, the effect of fire retardant on the combustion of wood was examined via X-ray computed tomography. XCT acquisitions provided 3D in-situ measurements of gas temperature and solid density. The results highlighted that FR coating only slightly affects the flaming regime, mainly through a minor reduction in heat release. However, after pyrolysis and flaming, a major reduction in the char oxidation was observed for samples coated with FR. The smoldering was almost entirely inhibited thanks to the growth of a protective dense char layer at the sample surface of about 1 mm thickness. This protective layer kept a constant density excess compared to the inside fuel during combustion, thus suggesting that the FR coating was mostly preserved at the sample surface. This behavior is consistent with the expected fire suppression mechanism of APP-based FRs at the temperatures measured. Only at the conditions considered with the highest oxygen content did the smoldering front penetrate through the protective char layer, at a location where the layer was relatively thin. Once a small breach was formed through the protective layer, the

interior of the char started to oxidize. The smoldering locally propagated near the breach, thereby releasing sufficient heat to enlarge the opening through the FR coating.

This study demonstrated the use of XCT to probe the shielding effect of FR coatings in suppressing fire. The results highlighted that detailed XCT measurements can be used to quantitatively analysis the efficacy and guide the design of FRs. In particular, the measurements indicated that APP-based FRs only slightly alter the amount of heat released during flaming at the conditions considered. However, these FRs largely reduced the char oxidation, thereby suggesting that FRs can effectively minimize spotting ignition due to firebrands, which is a significant mechanism of fire spread [11].

5. Acknowledgements

This research was supported by the NSF (Award No. CBET-1800906). Anthony C. Yu and Prof. Eric Appel are acknowledged for providing the Phos-Chek solution used in this work.

6. References

[1] E. Hirsch, and I. Koren, Record-breaking aerosol levels explained by smoke injection into the stratosphere, Science 371.6535 (2021), 1269–1274.
[2] R.K. Miller, C.B. Field, and K.J. Mach, Barriers and enablers for prescribed burns for wildfire management in California, Nat. Sustain. 3.2 (2020), 101–109.
[3] C.Y. Anthony, H.L. Hernandez, A.H. Kim, L.M. Stapleton, R.J. Brand, E.T. Mellor, C.P. Bauer, G.D. McCurdy, A.J. Wolff III, D. Chan, C.S. Criddle, J.D. Acosta, and E.A. Appel, Wildfire prevention through prophylactic treatment of high-risk landscapes using viscoelastic retardant fluids, Proc. Natl. Acad. Sci. 116.42 (2019) 20820–20827.
[4] S.T. Lazar, T.J. Kolibaba, and J.C. Grunlan, Flame-retardant surface treatments, Nat. Rev. Mater. 5.4 (2020), 259–275.
[5] J. Zhang, A.R. Horrocks, and M.E. Hall, The flammability of polyacrylonitrile and its copolymers IV. The flame retardant mechanism of ammonium polyphosphate, Fire Mater. 18.5 (1994), 307–312.
[6] G. Camino, L. Costa, and L. Trossarelli, Study of the mechanism of intumescence in fire retardant polymers: Part V—Mechanism of formation of gaseous products in the thermal degradation of ammonium polyphosphate, Polym. Degrad. Stab. 12.3 (1985), 203–211.
[7] K.S. Lim, S.T. Bee, L.T. Sin, T.T. Tee, C.T. Ratnam, D. Hui, and A.R. Rahmat, A review of application of ammonium polyphosphate as intumescent flame retardant in thermoplastic composites, Compos. B. Eng. 84 (2016), 155–174.
[8] J. Green, A Review of Phosphorus-Containing Flame Retardants, J. Fire Sci. 10.6 (1992), 470–487.
[9] E. Boigné, P. Muhunthan, D. Mohaddes, Q. Wang, S. Sobhani, W. Hinshaw, and M. Ihme, X-ray computed tomography for flame-structure analysis of laminar premixed flames, Combust. Flame 200 (2019), 142–154.
[10] E. Boigné, N.R. Bennett, A. Wang, K. Mohri, and M. Ihme, Simultaneous in-situ measurements of gas temperature and pyrolysis of biomass smoldering via X-ray computed tomography, Proc. Combust. Inst. 38 (2021) In press.
[11] S.L. Manzello, S. Suzuki, M.J. Gollner, A.C. Fernandez-Pello, Role of firebrand combustion in large outdoor fire spread, Prog. Energy Combust. Sci. 76 (2020), 100801.